Fundamental limit for integrated atom optics with Bose-Einstein condensates

Weiping Zhang,[1,2] Ewan M. Wright,[1] Han Pu,[1] and Pierre Meystre[1]
[1]*Optical Sciences Center, University of Arizona, Tucson, Arizona 85721, USA*
[2]*Department of Physics, Tsinghua University, Beijing, 100084, China*
(Received 4 April 2003; published 15 August 2003)

The dynamical response of an atomic Bose-Einstein condensate manipulated by an integrated atom-optics device, such as a microtrap or a microfabricated waveguide, is studied. We show that when the miniaturization of the device enforces a sufficiently high condensate density, three-body interactions lead to a spatial modulational instability that results in a fundamental limit on the coherent manipulation of Bose-Einstein condensates.

DOI: 10.1103/PhysRevA.68.023605 PACS number(s): 03.75.Kk, 67.40.Db

I. INTRODUCTION

The central idea of integrated atom optics is to miniaturize the size of active and passive atom-optical components, such as atom lasers, wave guides, beam splitters, and interferometers, and to combine them in integrated devices [1–12]. Potential future applications include hand-carried high-precision measurement devices such as gravimeters and gyroscopes. Integrated atom-optical chips may also prove useful to control neutral atoms in integrated and scalable microtrap arrays for quantum information processing. For example, microfabricated atom-optical components can be fabricated with current-carrying wires or microstructured surfaces, combined with homogeneous magnetic bias fields and periodically magnetized substrates. Optical fields or electric fields may also be involved in the hybrid construction of such devices.

However, the future of integrated atom optics still depends on finding solutions of a number of both technical and fundamental issues. For example, it will be essential to maintain the coherence of the matter waves to be manipulated, a step still to be demonstrated in waveguide-based beam splitters. Atoms confined in wire-based microtraps on atom chips face a relatively noisy environment, due e.g. to the heating from the chip substrate, which can cause the decoherence of atomic matter wave [13]. In addition, fluctuating currents in microwires may perturb the atoms when they are brought near its surface. Recent experiments have revealed the fragmentation of atomic Bose-Einstein condensates (BECs) confined in wire-based microtraps when the atom-surface distance is reduced to micrometer scale [10–12], and the experimental data seems to support the argument that the fluctuating currents in the wire and corrugations due to imperfect microfabrication are responsible for that fragmentation.

While such experiments illustrate the technical limitations for the coherent control of atoms in the microtraps, it can be hoped that these will be eliminated by better engineering solutions. In addition, though, it is also important to understand the fundamental limitations to integrated atom optics. For example, the strong compression typical of microtraps or waveguides can significantly increase the density of the atomic BECs, thereby enhancing inelastic collisions and resulting in a fundamental source of decoherence that reduces the lifetime of the confined BECs [10].

In this paper, we discuss an additional effect that limits the coherent control of atomic BECs in microtraps or microfabricated waveguides. Specifically, we show that when the miniaturization of the device results in a sufficiently high condensate density, three-body interactions lead to a spatial modulational instability that leads to the fragmentation of the condensate, thereby imposing a fundamental limit on the densities that can be stably propagated and manipulated in atomic waveguides.

The paper is organized as follows: Section II introduces our model and establishes the notation. Section III uses a linear stability analysis to show analytically the existence of a modulational instability in the condensate dynamics when three-body collisions become important. Section IV presents the results of selected numerical simulations that confirm the analytical predictions and show the onset of condensate fragmentation. Section V expands our analysis and presents arguments that reinforce the conclusions of the numerical simulations and argue that the modulational instability eventually leads to a collapse of the condensate. Finally, Sec. VI is a summary and outlook.

II. THE MODEL

For concreteness, we consider in this paper an atomic waveguide resulting from the combination of a current-carrying wire (for instance) electroplated on a substrate, and a static, homogeneous bias magnetic field $B_{\rm bias}$ [10] perpendicular to the conductor. Assuming a linear wire, the distance d of the waveguide to the chip surface is

$$d=\left(\frac{\mu_0}{2\pi}\right)\frac{I}{B_{\rm bias}}, \tag{1}$$

where μ_0 is the vacuum permeability and I the current through the wire. Since the guide height can be reduced using smaller currents or stronger bias field, the setup is ideal for the requirement of miniaturization in integrated atom optics.

The radial oscillation frequency of this trap is

$$\omega_r=\frac{2\pi}{\mu_0}\sqrt{\frac{\mu_B g_F m_F}{mB_0}}\frac{B_{\rm bias}^2}{I}, \tag{2}$$

where μ_B is the Bohr magneton, g_F and m_F the gyromagnetic ratio and magnetic moment of the hyperfine state of the alkali metal atoms of mass m being trapped, and we have assumed that the axial confinement of the atoms is achieved by a Ioffe-Pritchard-type trap that provides a field B_0 in the center of the trap.

Since the radial oscillation frequency ω_r scales as B_{bias}^2/I, any miniaturization of the trap achieved through a reduction of d results in an increase of ω_r, and hence in the density of the confined condensate. The closer to the chip surface the condensate is brought, the higher its density. In some of the present experiments, the condensate densities can already reach values in excess of 1×10^{15} cm^{-3}. For such high densities, the effects of three-body interactions on the dynamics of BECs are expected to become important. Our goal in this paper is to understand their impact on the dynamics of the guided condensate.

Our starting point is the three-dimensional Gross-Pitaevskii equation for the wave function $\Psi(\mathbf{r},t)$ of a trapped condensate, generalized to include three-body interactions,

$$i\hbar\frac{\partial\Psi}{\partial t}=\left[-\frac{\hbar^2}{2m}\nabla^2+\frac{1}{2}m\omega_z^2[\xi^2(t)r^2+z^2]-\mu\right]\Psi + \hbar g_2 N|\Psi|^2\Psi+\hbar g_3 N^2|\Psi|^4\Psi. \tag{3}$$

Here μ is the chemical potential, g_2 and g_3 measure the strength of the two-body and three-body interactions, respectively, $\Psi(\mathbf{r},t)$ is normalized to unity and N is the number of atoms in the condensate. We have also introduced the dimensionless ratio

$$\xi(t)=\omega_r(t)/\omega_z, \tag{4}$$

which determines the strength of the transverse confinement relative to the longitudinal trapping. [We allow $\xi(t)$ to be time dependent to include possible time variations of bias magnetic field B_{bias} or of the current I, and hence of ω_r.]

In the following, we assume that the microtrap is operating in the regime of tight transverse confinement, $\xi(t)\gg1$ and also that the transverse trapping potential is much larger than the interatomic interaction. We further assume that the time variation of $\omega_r(t)$ is slow enough so that the transverse profile of the BEC adiabatically follows the ground transverse oscillator state

$$\phi_0(r,t)=\sqrt{\frac{1}{\pi l_r^2(t)}}e^{-r^2/2l_r^2(t)}, \tag{5}$$

with $l_r(t)=\sqrt{\hbar/m\omega_r(t)}$.

We can then proceed by approximating the condensate wave function $\Psi(\mathbf{r},t)$ as

$$\Psi(\mathbf{r},t)\approx u(z,t)\phi_0(r,t)\exp\left[-i\int^t dt'\,\omega_r(t')\right], \tag{6}$$

where it is understood that the radial wave function $\phi_0(r,t)$ contains only slow time variations, and the envelope function $u(z,t)$ incorporates all other time variations. We then obtain the approximate equation for the envelope function

$$i\hbar\frac{\partial u}{\partial t}=\left[-\frac{\hbar^2}{2m}\frac{\partial^2}{\partial z^2}+\frac{1}{2}m\omega_z^2z^2-\mu\right]u+\hbar g_{2,z}(t)|u|^2u + \hbar g_{3,z}(t)|u|^4u, \tag{7}$$

where the reduced interatomic interaction coefficients $g_{2,z}$ and $g_{3,z}$ are

$$g_{2,z}(t)=g_2N\int 2\pi r dr|\phi_0(r,t)|^4=\left(\frac{g_2N}{2\pi l_z^2}\right)\xi(t),$$

$$g_{3,z}(t)=g_3N^2\int 2\pi r dr|\phi_0(r,t)|^6=\left(\frac{g_3N^2}{3\pi^2 l_z^4}\right)\xi^2(t), \tag{8}$$

where $l_z=\sqrt{\hbar/m\omega_z}$. From these definitions, we see that the reduced two-body interaction coefficient varies linearly with the transverse oscillator frequency or the ratio $\xi(t)=\omega_r(t)/\omega_z$, whereas the three-body coefficient scales as $\xi^2(t)$. This implies that the relative significance of two- and three-body interactions depends on the level of transverse confinement.

For alkali metal atoms, the two-body interaction coefficient has fully been determined by experiments. Although information for three-body interactions is still sketchy, recent theoretical studies have provided a way to estimate the three-body interaction coefficient g_3 [14–18]. For rubidium atoms, it may be expected to be negative, with $|g_3|$ of the order of 10^{-26}–10^{-27} cm^6/s. With this in mind, we focus our discussion on atoms with repulsive two-body interactions ($g_2>0$) and attractive three-body interactions ($g_3<0$).

III. MODULATIONAL INSTABILITY

To expose the basic modulational instability that arises at high densities, we first consider the case where the longitudinal trapping potential is switched off, the transverse trapping is fixed, so that $\xi\gg1$ is constant, and the condensate has a homogeneous longitudinal distribution u_0 over a length L. The chemical potential is then $\mu=\hbar g_{2,z}|u_0|^2-\hbar|g_{3,z}||u_0|^4$.

We are interested in the condensate dynamics in the presence of the attractive three-body interaction. For this purpose, we first carry out a linear stability analysis by setting

$$u(z,t)=[u_0+\delta u(z,t)]e^{-i\mu t/\hbar}, \tag{9}$$

and looking at longitudinal excitations of the form

$$\delta u(z,t)=\sum_k\,[\alpha_kU_k(z)e^{-i\nu_kt}-\alpha_k^\dagger V_k(z)^*e^{i\nu_kt}].$$

Substituting Eqs. (9) and (10) into Eq. (7), we obtain

$$\left(-\frac{\hbar}{2m}\frac{\partial^2}{\partial z^2}+\eta\right)U_k-\eta V_k=\nu_kU_k,$$

$$\left(-\frac{\hbar}{2m}\frac{\partial^2}{\partial z^2}+\eta\right)V_k-\eta U_k=-\nu_kU_k, \tag{10}$$

where we have defined

$$\eta = g_{2,z}|u_0|^2 - 2|g_{3,z}||u_0|^4. \tag{11}$$

Considering plane-wave excitations $U_k = (1/L)\exp(ikz)$ and $V_k = (1/L)\exp(-ikz)$, Eq. (10) gives the excitation frequencies

$$\nu_k = \sqrt{\frac{\hbar k^2}{2m}\left(\frac{\hbar k^2}{2m} + 2\eta\right)}, \tag{12}$$

which reduce to the familiar Bogoliubov spectrum in the absence of three-body excitations. In that limit, the excitation energies are always positive and the condensate is stable. However, the situation changes completely when $g_{2,z} < 2|g_{3,z}||u_0|^2$, or $\eta < 0$, in which case the excitation energies can become imaginary. Physically, such complex frequencies imply that spatially modulated perturbations can grow with time, that is, a modulational instability may occur. The maximum gain occurs for the wave number k such that $\hbar k^2/2m = |\eta|$, which yields the spatial period of the most unstable wave as $L_m = \sqrt{2\pi^2\hbar/(m|\eta|)}$. Provided that the length of the BEC satisfies $L > L_m$, it will then become modulationally unstable due to the attractive three-body interactions. As a result, a spatial inhomogeneity will develop in the condensate density profile along the z axis. Three-body interactions impose a fundamental limit on the linear densities that can be stably propagated and manipulated in the waveguide.

Consider a ^{87}Rb BEC as an example. The two-body interaction coefficient of ^{87}Rb is $g_2 = 4\pi\hbar a_s/m \sim 4.95\times 10^{-11}$ cm^3/s. The theoretical estimate of the three-body interaction coefficient is $|g_3| \sim 10^{-26} - 10^{-27}$ cm^6/s. The onset of the modulational instability occurs then at $|g_3|\rho_0 \sim g_2/2$, with ρ_0 being the three-dimensional density of the condensate. This yields a threshold density of the order of 10^{15}–10^{16} cm^{-3}, beyond which the condensate becomes dynamically unstable. We remark that such densities might have already been achieved in recent experiments. The corresponding modulational length is on the order of a few microns.

IV. NUMERICAL SIMULATIONS

In this section, we present numerical simulations that illustrate the effect of the modulational instability on the condensate dynamics. In particular, we consider the case in which the magnitude of the bias magnetic field $B_{\rm bias}$ is decreased to lower a magnetically trapped gas towards the atom chip surface. We assume that the initial trapped gas is stable against modulational instabilities. As the condensate approaches the surface of the chip, its linear density increases concomitantly with the increasing transverse trapping frequency. The gas can then become modulationally unstable. Our numerics give illustrative examples of the development of this instability.

For convenience of numerical calculation, we introduce the dimensionless variables $\tau = \omega_z t, \zeta = z/l_z$, and $\Phi(\zeta,\tau) = \sqrt{l_z}u$, to yield

$$i\frac{\partial\Phi}{\partial\tau} = \left(-\frac{1}{2}\frac{\partial^2}{\partial\zeta^2} + \frac{1}{2}\zeta^2\right)\Phi + \beta_2 f(\tau)|\Phi|^2\Phi + \beta_3 f^2(\tau)|\Phi|^4\Phi, \tag{13}$$

where

$$\beta_2 = \frac{(g_2 N/2\pi l_z^3)}{\hbar\omega_z}\xi_0, \quad \beta_3 = \frac{(g_3 N^2/3\pi^2 l_z^6)}{\hbar\omega_z}\xi_0^2. \tag{14}$$

Here we have written

$$\xi(\tau) = \omega_r(\tau)/\omega_z = \xi_0 f(\tau),$$

$\xi_0 = \omega_r(0)/\omega_z$ being the initial ratio of the transverse and longitudinal trapping frequencies. The function $f(\tau)$ incorporates the time variation of the magnetic bias field. We choose ξ_0 such that the three-body interactions are initially negligible for the trapped gas and the condensate is initially stable. As it is lowered the transverse trapping frequency and linear density increase, and so $f(\tau)$ increases from unity. We note from Eq. (13) that the two-body interaction term is proportional to $f(\tau)$ and the three-body term is proportional to $f^2(\tau)$, so that as the BEC approaches the surface, the importance of three-body interactions increases, as we have seen.

We take parameters appropriate to a ^{87}Rb BEC composed of $N = 10^4$ atoms, $m = 1.44\times 10^{-25}$ kg, $g_2 = 4.95\times 10^{-11}$ cm^3/s, $g_3 = -4\times 10^{-26}$ cm^6/s, with a longitudinal trap frequency $\omega_z = 2\pi\times 14$ rad/s, giving $l_z = 2.8$ μm [20]. With these parameters we find $\beta_2 = 375$ and $|\beta_3| = 270$. We choose the initial transverse trapping frequency such that $\xi_0 = \omega_r(0)/\omega_z = 10$, and assume a linear ramp of $\omega_r(\tau)$, $f(\tau) = 1 + \alpha\tau$, where $\alpha = 1.5$. The initial macroscopic wave function $\Phi(\zeta,0)$ is chosen as the ground state $\chi(\zeta)$ of the trap, neglecting the three-body interactions. An approximation to the ground state is obtained in the Thomas-Fermi approximation by setting $\Phi(\zeta,\tau) = \exp(-i\gamma\tau)\chi(\zeta)$ and imposing the normalization condition $\int d\zeta|\chi(\zeta)|^2 = 1$ to yield

$$|\chi(\zeta)|^2 = \frac{1}{\beta_2}(\mu - \zeta^2/2)\,\theta(\mu - \zeta^2/2), \quad \gamma = \frac{1}{2}\left(\frac{3\beta_2}{2}\right)^{2/3}, \tag{15}$$

where $\theta(y)$ is the Heaviside step function. Our condition that the transverse trapping frequency varies slowly compared to the longitudinal dynamics requires $\gamma \gg \alpha$, which is satisfied by our chosen parameters.

Figure 1 shows the evolution of the scaled linear density $|\Phi(\zeta,\tau)|^2$ versus ζ and τ, in the absence of ramping of the transverse trapping frequency $(\alpha = 0)$. The density profile remains intact in time, except for a small modulation that arises from the fact that the initial macroscopic wave function is the ground state without the three-body interactions, whereas the numerical simulation in Fig. 1 incorporates the three-body interactions. This results in some small rearrangement of the density profile. The robustness of the density profile to the inclusion of the three-body interactions shows that the initial state is stable and the three-body effects are

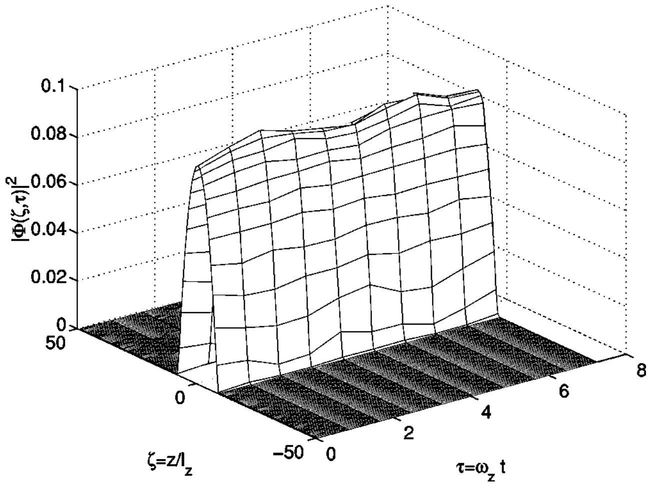

FIG. 1. Scaled density $|\Phi(\zeta,\tau)|^2$ versus ζ and τ for the case with no ramping of the transverse trapping frequency ($\alpha=0$).

not important for these initial parameters. This also justifies our use of this particular initial wave function.

This result should be compared and contrasted with Fig. 2, which shows the evolution of the scaled linear density $|\Phi(\zeta,\tau)|^2$ versus τ for $\tau=0\rightarrow7.5$ for a situation where the transverse trapping frequency is ramped ($\alpha=1.5$). As the transverse trapping frequency $\xi(\tau)=\omega(\tau)/\omega_z=10\times(1+1.5\tau)$ increases in time, the initial effect is a broadening of condensate width. This is a consequence of the fact that the dominant repulsive two-body interactions are becoming stronger. The density undulations, seen in Fig. 2, arise from the interplay between the attractive harmonic trapping and the increasing two-body repulsion.

As time increases further, the role of the attractive three-body interactions starts to become important, with the onset of the modulational instability increasing for $\tau>7.5$. Figure 3 shows the development of the instability around the center of the trap at the dimensionless times $\tau=7.64$ (dotted line), $\tau=7.68$ (dashed line), and $\tau=7.72$ (solid line). A spatial modulation of the condensate density of period $L/l_z\simeq0.8$ is

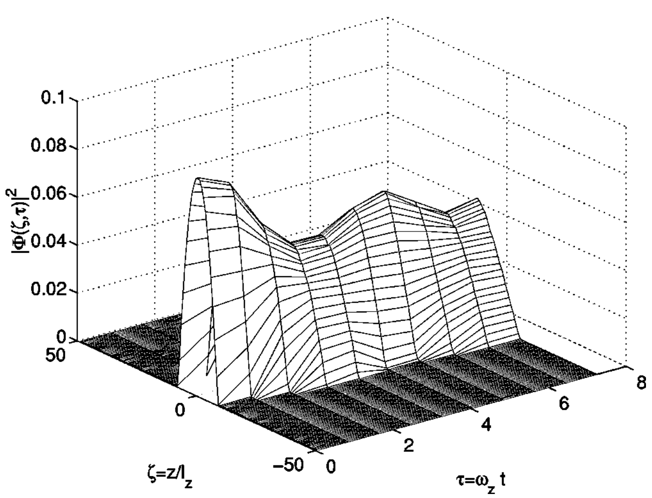

FIG. 2. Scaled density $|\Phi(\zeta,\tau)|^2$ versus ζ and τ for the case with ramping of the transverse trapping frequency ($\alpha=1.5$).

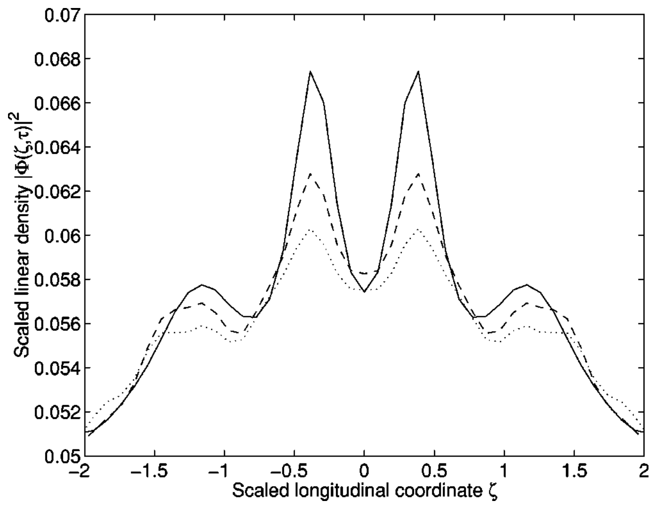

FIG. 3. Scaled density $|\Phi(\zeta,\tau)|^2$ versus ζ for times $\tau=7.64$ (dotted line), $\tau=7.68$ (dashed line), and $\tau=7.72$ (solid line).

clearly seen to be developing, resulting in a fragmentation of the density profile of the trapped gas.

One can compare this period with the analytical predictions of Sec. III by treating the center of the BEC as approximately homogeneous. Converting to dimensionless units, the period of the most unstable wave vector becomes

$$\frac{L_m}{l_z}\simeq\sqrt{\frac{2\pi^2}{|\beta_2 f_{\max}n_c-2|\beta_3|f_{\max}^2n_c^2|}}, \tag{16}$$

where $f_{\max}=13$ is the value of $f(\tau=8)$ for times in the vicinity where the instability develops, and $n_c\simeq0.06$ is the value of the scaled linear density at the trap center. From this we obtain $L_m/l_z\approx0.74$, in reasonable agreement with the period 0.8 between the peaks in Fig. 3. We remark that the threshold for the modulational instability occurs when the denominator in Eq. (16) vanishes, that is, $|\beta_2 f_{\max}n_c-2|\beta_3|f_{\max}^2n_c^2|=0$.

For times $\tau>8$ the main density peaks generated by the modulational instability in Fig. 3 continue to grow, and the numerical simulations quickly break down thereafter. Indeed, the numerical solutions indicate that the density peaks are undergoing a collapse whereby the density locally increases towards infinity within a finite time. Abdullaev *et al.* [21] have previously shown that a collapse is possible in a trapped gas with repulsive two-body interactions. This collapse is analogous to the corresponding case for two- or three-dimensional condensates, where a collapse occurs for condensates large enough so that the attractive two-body interactions overcome the "quantum pressure" associated with the trap ground state. By contrast, the present system is effectively one-dimensional (in ζ), but with a combination of repulsive two-body interactions and attractive three-body interactions, and it is the competition between these two mechanisms that leads to condensate collapse for sufficiently high densities. This places a fundamental limitation on the linear densities that can be stably sustained in atom microtraps and waveguides.

In practice, the predicted collapse will be regularized by some additional physical process, such as three-body losses as in the case of higher-dimensional collapse in the Bose-Novae. We conjecture that a form of soliton turbulence will ensue [22,23]. In addition, as the linear density continues to grow the mean-field energy will eventually exceed the transverse mode energy, in which case multiple transverse modes will be excited thereby arresting the collapse.

We point out that the above results are based on the assumption that the Gross-Pitaevskii equation is valid to describe the dynamics of the confined one-dimensional Bose-Einstein condensate. In fact, we can assess the validity of our use of the Gross-Pitaevskii equation to model the confined one-dimensional BEC by examining the dimensionless parameter $\gamma = mg/\hbar^2 n$, where $g = \hbar g_{2,z}/N = (\hbar g_2/2\pi l_z^2)\xi$ is the effective one-dimensional coupling constant and $n \approx \rho_0 \pi l_z^2$ is the linear density [24,25]. In particular, previous theoretical studies have shown that $\gamma \ll 1$ corresponds to the Gross-Pitaevskii regime, whereas $\gamma \gg 1$ corresponds to the strongly interacting Tonks-Girardeau regime [24,25]. For our case we obtain $\gamma = (m g_2 \xi / 2\pi^2 \hbar l_z^4 \rho_0)$, which for the previously stated ^{87}Rb parameters, $\xi = 100$, and $\rho_0 \simeq 10^{15}$ cm^{-3}, gives $\gamma \simeq 10^{-5}$, so we are well justified in using the Gross-Pitaevskii equation. Furthermore, the simulations presented here well obey the diluteness condition $\rho_0 a^3 \ll 1$, with a the scattering length, since $1/a^3 \simeq 10^{19}$ cm^{-3} which is a very large density compared to those considered here in the atomic BEC experiments.

V. COLLAPSE AND MODULATIONAL INSTABILITY

In this section, we present a discussion that reinforces the argument that the modulational instability eventually leads to condensate collapse. We proceed by reexamining the generalized Gross-Pitaevskii equation (13), which can be interpreted as resulting from the effective potential

$$U_{eff}(\zeta) = \frac{1}{2}\zeta^2 + \beta_2 f|\Phi|^2 + \beta_3 f^2 |\Phi|^4. \tag{17}$$

Consider a normalized Gaussian approximate trial solution of width l

$$\Phi(\zeta) \approx \left(\frac{1}{\pi l^2}\right)^{1/4} e^{-\zeta^2/(2l^2)}, \tag{18}$$

which relates the peak density $|\Phi(0)|^2$ at trap center to l via

$$n_c = |\Phi(0)|^2 = 1/\sqrt{\pi l^2}. \tag{19}$$

Near the center, and evaluating the potential for parameters $f_{\max}, n_c$ in the vicinity of where the modulational instability develops, we have

$$U_{eff}(\zeta) \approx (\beta_2 f_{\max} n_c - |\beta_3| f_{\max}^2 n_c^2) + \frac{\zeta^2}{l^2}\left(\frac{l^2}{2} - \beta_2 \pi f_{\max} n_c + 2|\beta_3| \pi f_{\max}^2 n_c^2\right) + \cdots . \tag{20}$$

We are interested in the term in large parenthesis, which controls the dominant confinement properties due to the combined effects of the linear trap and two- and three-body interactions. At densities low enough for the two-body interactions to dominate over the three-body processes, the two-body collisions oppose the focusing of the trap, and their balance produces a stable and confined solution. In contrast, when attractive three-body interactions dominate, both the trap and the three-body interactions work to compress the density, causing a strong focusing of the density distribution and collapse. We, therefore, anticipate that the crossover from stability to collapse will occur when the two- and three-body focusing terms in the large parentheses cancel each other,

$$\beta_2 \pi f_{\max} n_c - 2|\beta_3| \pi f_{\max}^2 n_c^2 = 0. \tag{21}$$

This coincides precisely with the modulational instability threshold from Eq. (16). Thus, the appearance of a modulational instability also signals that the condensate will collapse if the trapped gas is too close to the atom chip surface. This conclusion is also in agreement with the results of Abdullaev *et al.* [21], regarding the stability of trapped gases. We remark that, although we have considered a magnetically trapped gas, the same conclusions clearly apply to an optically trapped gas at sufficiently high densities.

We can also use a variational approach to treat the collapse of the condensate more rigorously. Consider Eq. (18) as the variational wave function with width l being the variational parameter. The energy functional associated with the dimensionless Schrödinger equation (13) is then given by

$$E(l) = \int dz \Phi(\zeta)\left[-\frac{1}{2}\frac{\partial^2}{\partial \zeta^2} + \frac{1}{2}\zeta^2 + \frac{1}{2}\beta_2 f |\Phi(\zeta)|^2 + \frac{1}{3}\beta_3 f^2 |\Phi(\zeta)|^4\right]\Phi(\zeta) = \frac{l^2}{4} + \frac{\mathcal{A}}{l} - \frac{\mathcal{B}}{l^2}, \tag{22}$$

where $\mathcal{A} = \beta_2 f/(2\sqrt{2\pi})$ and $\mathcal{B} = |\beta_3| f^2/(3\sqrt{3}\pi) - 1/4$.

From Eq. (22), we have $E(l) \to -\infty$ as $l \to 0$ provided that $\mathcal{B} > 0$. This means that under such a condition, the condensate is not stable against collapse. However, the system can still become metastable if $E(l)$ possesses a local minimum at finite l. This is analogous to the metastability of an attractive condensate with a sufficiently small number of atoms [19]. The condition for the existence of a local minimum is $dE(l)/dl = 0$ and $d^2E(l)/d^2 l > 0$, which yields

$$F(l) \equiv \frac{1}{2} l^4 - \mathcal{A} l + 2\mathcal{B} = 0,$$

$$l > \frac{8\mathcal{B}}{3\mathcal{A}}.$$

It can be shown that the above conditions are satisfied if and only if

$$F\left(\frac{8\mathcal{B}}{3\mathcal{A}}\right) = \frac{1}{2}\left(\frac{8\mathcal{B}}{3\mathcal{A}}\right)^4 - \frac{2}{3}\mathcal{B} < 0. \tag{23}$$

The local minimum vanishes when the above inequality becomes an equality. For the parameters of our numerical calculations, this happens at $\tau \approx 8.4$, which is in reasonable agreement with the onset of collapse $\tau > 8$ found in the simulations. This not only further establishes the connection between the modulational instability and the condensate collapse, but also provides the condition for the threshold of the instability through Eq. (23).

VI. SUMMARY AND CONCLUSIONS

Generic microtraps and atomic waveguides based on chip technology are characterized by an increased level of transverse confinement, and hence increased atomic density, as their distance from the chip is reduced. As a result, the three-body collisions become increasingly important. We have shown that for attractive collisions they can lead to a modulational instability in the dynamics of the condensate, and its eventual collapse, in agreement with the prior work of Abdullaev *et al.* [21] on the stability of trapped gases. The physics underlying this collapse, which involves the competition between repulsive two-body collisions and attractive three-body collisions, is reminiscent of the physics underlying the collapse of condensates with attractive two-body interactions, except that in that latter case, the competition is between the effect of collisions and the quantum pressure associated with the trap ground state. In both cases, though, the competition leads to a fundamental limit on the size of condensates that can be stably trapped and coherently manipulated, since the modulational instability and collapse correspond to a form of spatial fragmentation that will persist for trapped gases even though current technical sources of noise are eliminated.

In addition to predicting a fundamental limit in integrated atom optics, the present study also opens up intriguing new directions of investigation. For instance, we recall that the use of Feshbach resonances to switch the sign of the scattering length from positive to negative has lead to the discovery of fascinating dynamical effects, such as Bose-Novae in the three-dimensional condensates. Similar studies, but in one dimension, should now become possible simply by modulating either the bias field B_{bias} or the current I in wire microtraps. In practice, the predicted collapse and the subsequent dynamics of the collapsing filaments will be regularized by some additional physical process, such as three-body losses as in the case of higher-dimensional collapse in the Bose-Novae, or excitation of higher-order transverse modes as the mean-field energy rises due to collapse. In future work, we shall investigate the detailed dynamics of this one-dimensional Bose-Novae beyond the initial growth of the modulational instability considered here.

ACKNOWLEDGMENTS

We gratefully acknowledge extended discussions with C. P. Search. This work was supported in part by the US Office of Naval Research under Contracts No. 14-91-J1205 and No. N00014-99-1-0806, by the National Science Foundation under Grant No. PHY98-01099, by the US Army Research Office, by the NASA Microgravity Fundamental Physics Program, and by the Joint Services Optics Program.

[1] J.D. Weinstein and K.G. Libbrecht, Phys. Rev. A **52**, 4004 (1995).
[2] J. Fortagh, A. Grossman, C. Zimmermann, and T.W. Hänsch, Phys. Rev. Lett. **81**, 5310 (1998).
[3] J. Reichel, W. Hänsel, and T.W. Hänsch, Phys. Rev. Lett. **83**, 3398 (1999).
[4] J.H. Thywissen, R.M. Westervelt, and M. Prentiss, Phys. Rev. Lett. **83**, 3762 (1999).
[5] D. Müller, D.Z. Anderson, R.J. Grow, P.D.D. Schwindt, and E.A. Cornell, Phys. Rev. Lett. **83**, 5194 (1999).
[6] N.H. Dekker *et al.*, Phys. Rev. Lett. **84**, 1124 (2000).
[7] E.A. Hinds, C.J. Vale, and M.G. Boshier, Phys. Rev. Lett. **86**, 1426 (2001).
[8] R. Folman, P. Krüger, C. Henkel, and J. Schmiedmayer, Adv. At., Mol., Opt. Phys. **48**, 263 (2002).
[9] E. Andersson *et al.*, Phys. Rev. Lett. **88**, 100401 (2002).
[10] J. Fortagh, H. Ott, S. Kraft, A. Güntherÿ, and C. Zimmermann, Phys. Rev. A **66**, 041604(R) (2002)
[11] A.E. Leanhardt, Y. Shin, A.P. Chikkatur, D. Kielpinski, W. Ketterle, and D.E. Pritchard, Phys. Rev. Lett. **90**, 100404 (2003).
[12] M.P.A. Jones, C.J. Vale, D. Sahagun, B.V. Hall, and E.A. Hinds, e-print quant-ph/0301018.
[13] C. Henkel, P. Krüger, R. Folman, and J. Schmiedmayer, Appl. Phys. B: Lasers Opt. **76**, 173 (2003).
[14] P.F. Bedaque, E. Braaten, and H.-W. Hammer, Phys. Rev. Lett. **85**, 908 (2000).
[15] E. Braaten and H.-W. Hammer, Phys. Rev. Lett. **87**, 160407 (2001).
[16] E. Braaten, H.-W. Hammer, and Thomas Mehen, Phys. Rev. Lett. **88**, 040401 (2002).
[17] Michael W. Jack, Phys. Rev. Lett. **89**, 140402 (2002).
[18] Thorsten Köhler, Phys. Rev. Lett. **89**, 210404 (2002).
[19] H. Shi and W. Zheng, Phys. Rev. A **55**, 2930 (1997); M. Ueda and A.J. Leggett, Phys. Rev. Lett. **80**, 1576 (1998).
[20] For numerical reasons, a small number of atoms is used here so that the threshold of the modulational instability occurs at a relatively small wave number and hence can be spatially resolved over the width of the condensate.
[21] F.Kh. Abdullaev, A. Gammal, L. Tomio, and T. Frederico, Phys. Rev. A **63**, 043604 (2001).
[22] V.E. Zakharov, A.N. Pushkarev, V.F. Shvets, and V.V. Yan'kov, JETP Lett. **48**, 83 (1988).
[23] S. Dyachenko, A.C. Newell, A.N. Pushkarev, and V.E. Zakharov, Physica D **57**, 96 (1992).
[24] M. Olshanii, Phys. Rev. Lett. **81**, 938 (1998).
[25] D.S. Petrov, G.V. Shlyapnikov, and J.T.M. Walraven, Phys. Rev. Lett. **85**, 3745 (2000).